Fe^{+2}/Fe^{+3} ions doping effect on magnetic properties of hydroxyapatite nanoparticles

V. Iannotti[a], G. Ausanio[a], L. Lanotte[a], K.N. Trohidou[b], A. Adamiano[c], M. Sandri[c], and A. Tampieri[c]

[a]CNR-SPIN and Department of Physics, University of Naples "Federico II", p.le V. Tecchio 80, I-80125 Napoli, Italy

[b]Institute of Nanoscience and Nanotechnology, NCSR 'Demokritos', aghia paraskevi, 15310 Athens, Greeece

[c]Institute of science and Technology for Ceramics – National Research Council, Faenza (RA) 48018, italy

101° Congresso Nazionale SIF,
Roma, Italia, 25 Settembre 2015

MOTIVATIONS

Letter to the Editor — *J. Cell. Mol. Med. Vol 19, No 8, 2015 pp. 2032-2035*

Iron-induced myocardial injury: an alarming side effect of superparamagnetic iron oxide nanoparticles

Toxicology Letters 203 (2011) 162–171

Contents lists available at ScienceDirect

Toxicology Letters

journal homepage: www.elsevier.com/locate/toxlet

Endothelial dysfunction and inflammation induced by iron oxide nanoparticle exposure: Risk factors for early atherosclerosis

Cell Biol Toxicol (2011) 27:333–342
DOI 10.1007/s10565-011-9191-9

Cytotoxicity, permeability, and inflammation of metal oxide nanoparticles in human cardiac microvascular endothelial cells

Cytotoxicity, permeability, and inflammation of metal oxide nanoparticles

Biol Trace Elem Res (2014) 159:416–424
DOI 10.1007/s12011-014-9972-0

Iron Oxide Nanoparticles Induce Oxidative Stress, DNA Damage, and Caspase Activation in the Human Breast Cancer Cell Line

Strategy to mitigate toxicity

Biomaterials 34 (2013) 9615–9622

Contents lists available at ScienceDirect

Biomaterials

journal homepage: www.elsevier.com/locate/biomaterials

Suppressing iron oxide nanoparticle toxicity by vascular targeted antioxidant polymer nanoparticles

Journal of Materials Chemistry B

PAPER

View Article Online
View Journal | View Issue

An intrinsically magnetic biomaterial with tunable magnetic properties

HYDROXYAPATITE: Why ?

1) Calcium phosphate has been well understood as bioactive and biodegradable material. Especially, hydroxyapatite [Ca10(PO4)6(OH)2, HA] is a chief inorganic component of hard tissue and exhibits excellent bone conductivity and biocompatibility;

2) It has been reported that the resolvability of HA decreased by addition of Fe, and HA is basically understood as a low degradable material in a body. Therefore, it is expected that non toxicity magnetic bead can be developed by addition of Fe to the HA structure.

3) **In this study, we doped Fe to the HA to use as a novel magnetic bead to control its action by magnetic field and investigated the effects of Fe doping on the crystal phase, microstructure and magnetic properties of HAP**

The structure of HA allows for substitution of the calcium sites by divalent or trivalent cations and the hydroxyl site by other anions.

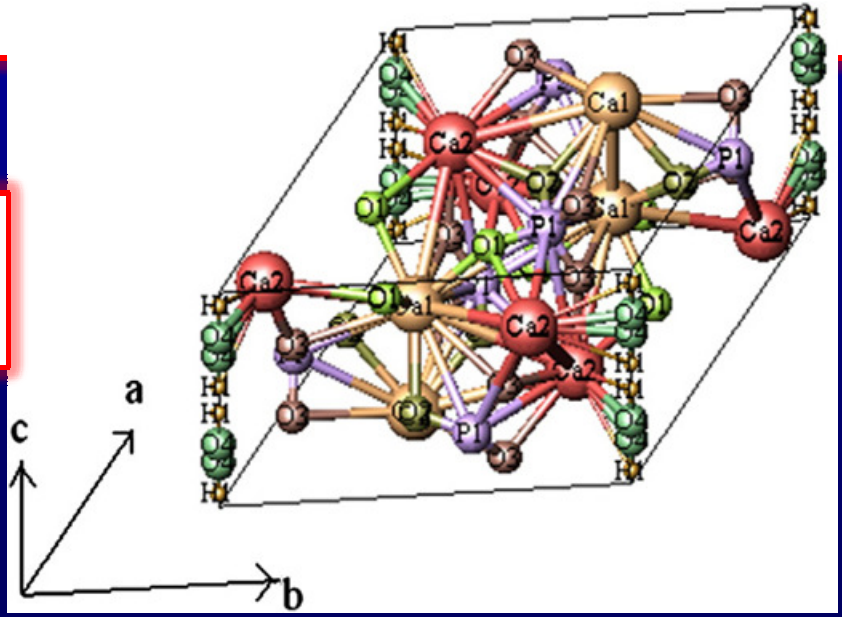

Flow Chart of the Synthesis Pathways Used for Obtaining the Different Particles

$Ca(OH)_2$

H_3PO_4 Dropwise addition → HAp

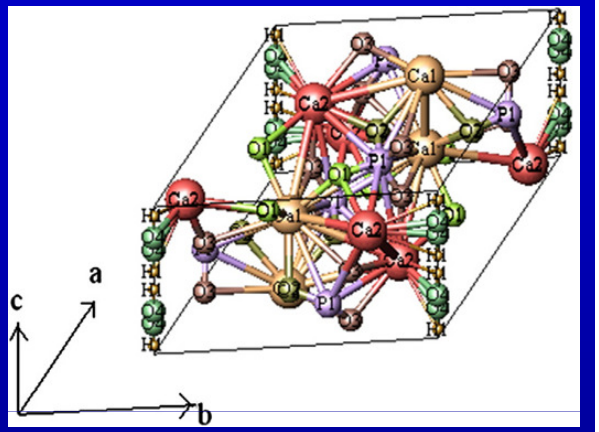

H_3PO_4, Fe^{2+}/Fe^{3+} Dropwise addition → FeHA3, FeHA2, FeHA

T = 45 °C

HAp = Control hydroxyapatite powder

FeHA = Fe^{+2+3}-doped hydroxyapatite nanoparticles powder

FeHA2 = Fe^{+2}-doped hydroxyapatite nanoparticles powder

FeHA3 = Fe^{+3}-doped hydroxyapatite nanoparticles powder

Structural Analysis: XRD

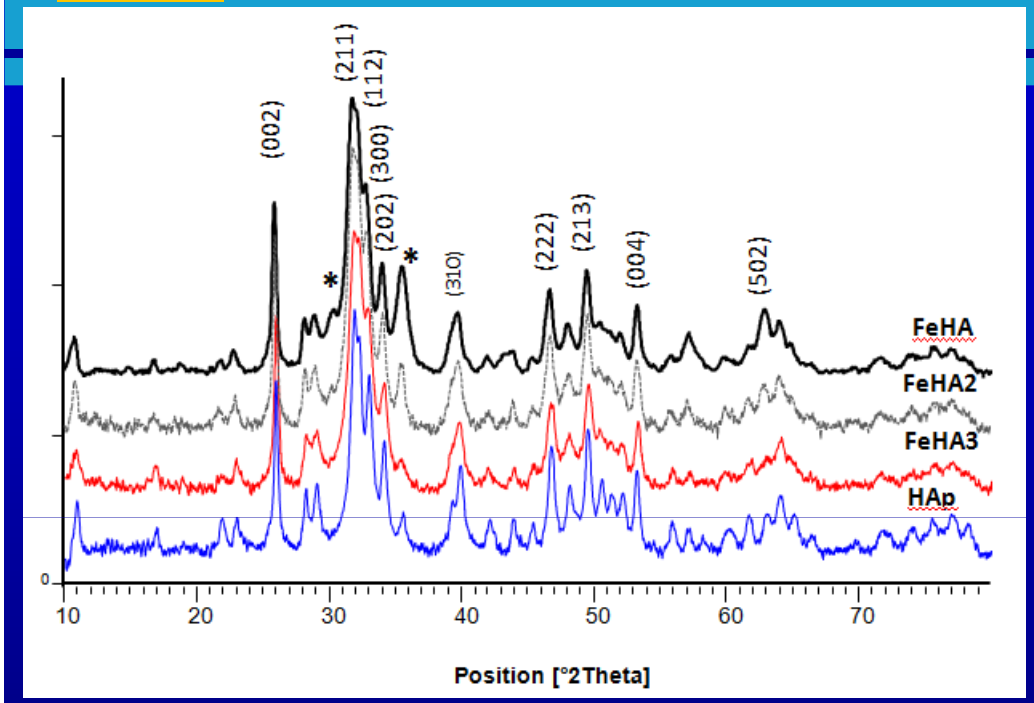

	HA	FeHA	FeHA2	FeHA3
HA (%)	100.0	95.6	96.5	100.0
Magnetite (%)	0.0	4.4	3.5	0.0
D (nm)	24.1	19.8	16.3	15.1
Cristallinity (%)	57	46	55	55
IR-SF	3.4	2.6	3.2	3.2

Phase composition and cell parameters calculated by Rietveld analysis of the XRD spectra. Infra-red splitting factor (IR-SF) was calculated by the FT-IR spectra.

- Presence of hydroxyapatite structure in HAp , FeHA, FeHA2 and FeHA3
- Presence of Magnetite/Maghemite as secondary phase in FeHA, FeHA2 , but not in FeHA3 ;
- XRD spectra reveal a low crystalline apatite with a crystallinity extent much lower for FeHA powders than the non-substitute HA, FeHA2 and FeHA3

FeHA: Chemical Analysis by ICP

Sample	Fe_{tot} (wt%)	Maghemite			HA					
		vol %	*wt%*	*Fe_{tot} wt%*	*Fe^{2+} (wt%)**	*Fe^{3}+ (wt%)*	*Fe^{3+}/Fe^{2+}*	*Fe/Ca % mol.*	*Ca/P mol.*	*(Fe+Ca)/P %mol.*
HA	-	-	-	-	-	-	-	-	1.67	-
FeHA	8.82± 0.19	2.7	4.4	3.08	3.6	2.14	0.59	16	1.41	1.64
FeHA2	10.13±0.11	2.1	3.5	2.45	4.3	3.38	0.79	20	1.45	1.74
FeHA3	4.32±0.05	0.0	0.0	0.0	X	4.32	X	10	1.62	1.78

Fe^{3+} was calculated as the difference between the total iron content detected by ICP-OES and the amount of Fe^{2+} detected by UV-VIS. Maghemite percentages were estimated by Rietveld refinement of the XRD spectra.

For FeHA and FeHA2 samples, the (Fe+Ca)/P molar ratios are 1.64 and 1.74, respectively, while the Ca/P molar ratios are lower than the stoichiometric HA one (1.67), giving an evidence of the replacement of Ca with Fe.

For FeHA3 sample, the (Fe+Ca)/P is 1.78, while the Ca/P molar ratio is closest to that of stoichiometric HA, indicating that Fe+3 ions do not compete efficiently with Ca ions for the occupation of HA lattice sites, substituting them to a lesser extent with respect to Fe+2 ions.

FeHA TEM Analysis

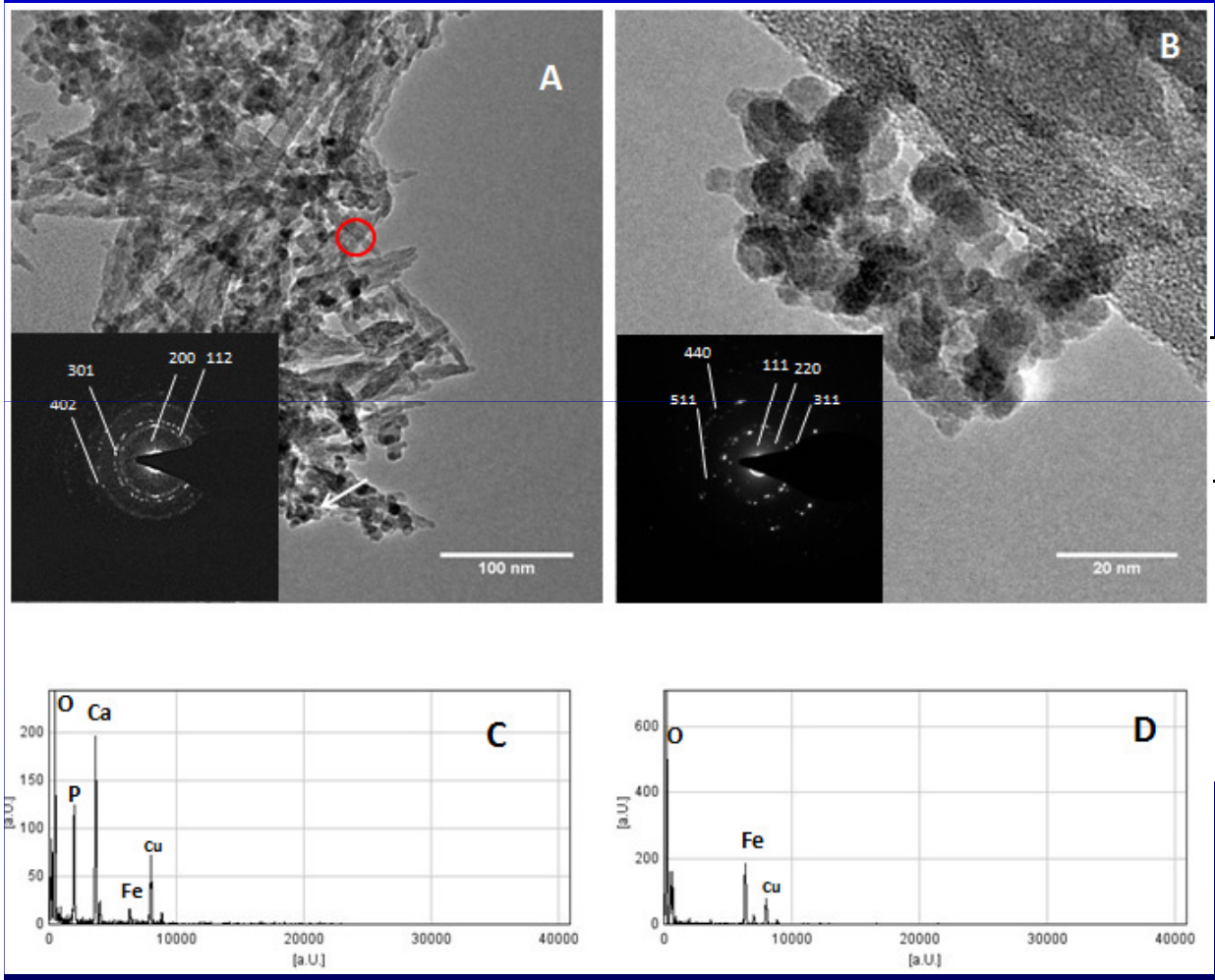

TEM pictures collected on FeHA, and the microanalysis spectrum depicted in figures C and D relative to figures A and B respectively.

Maghemite Planes	d-spacing (Å)	HA Planes	d-spacing (Å)
111	4.698	200	4.108
220	2.913	211	2.797
311	2.585	301	2.485
511	1.661	402	1.745

Magnetite/Maghemite and hydroxyapatite d-spacing calculated from selected area diffraction pattern.

FeHA2 and FEHA3 TEM Analysis

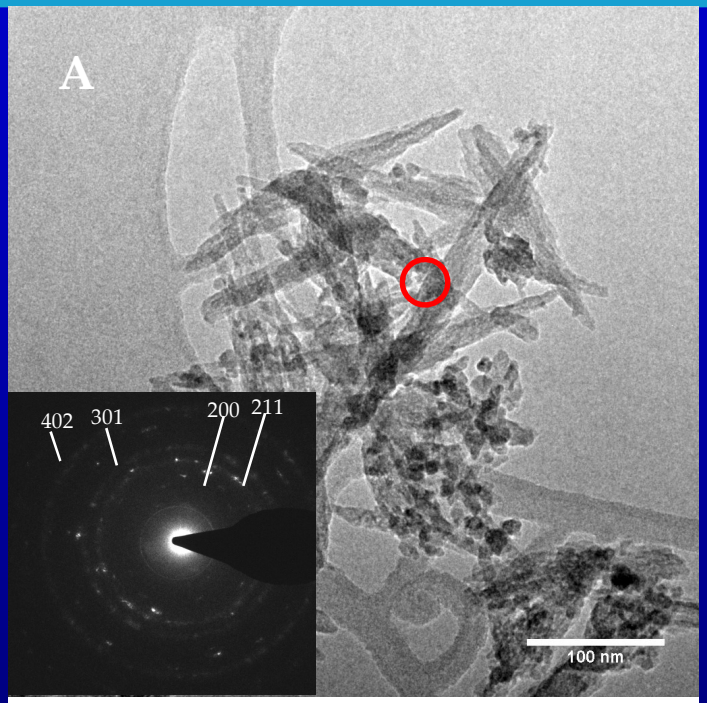

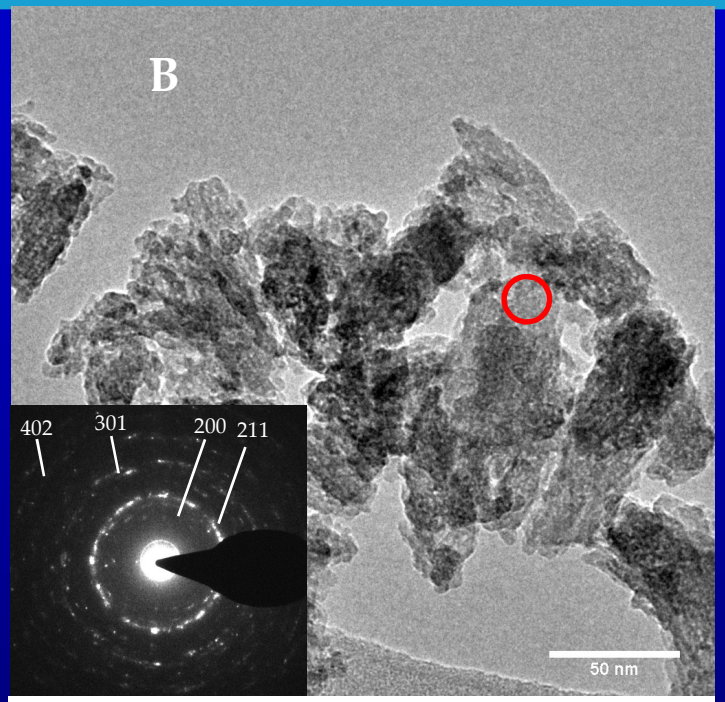

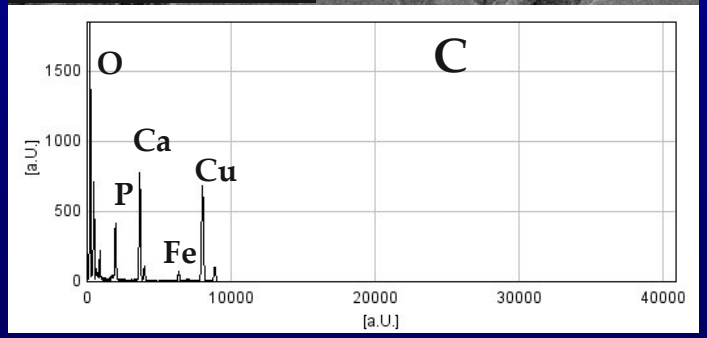

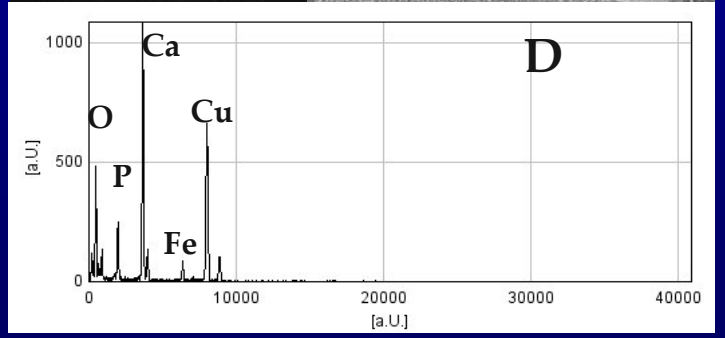

TEM pictures collected on FeHA2 (A) and FEHA3 (B), and the microanalysis spectrum depicted in figures C and D relative to figures A and B respectively.

STEM Analysis

FeHA

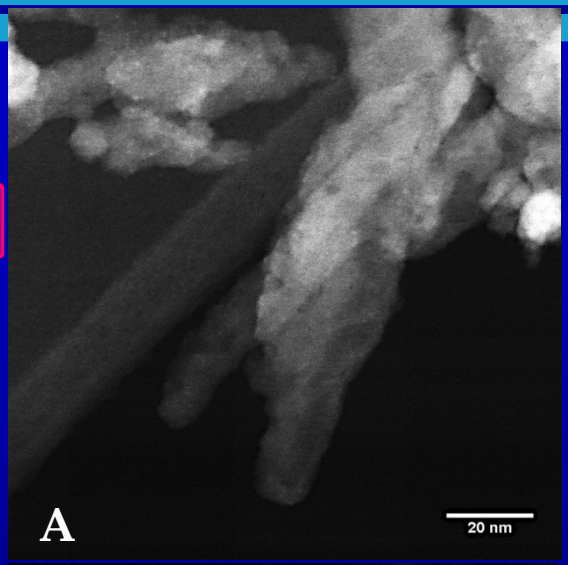

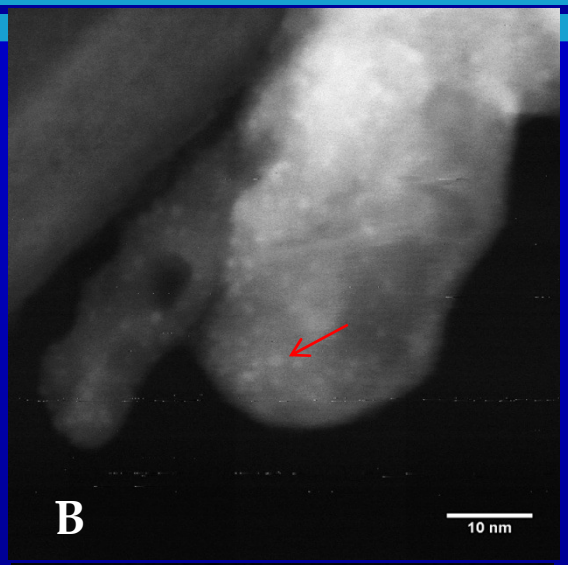

STEM pictures of FeHA at increasing magnification (B). In picture iron rich areas (brighter spots) are highlighted by a red arrow.

FeHA2

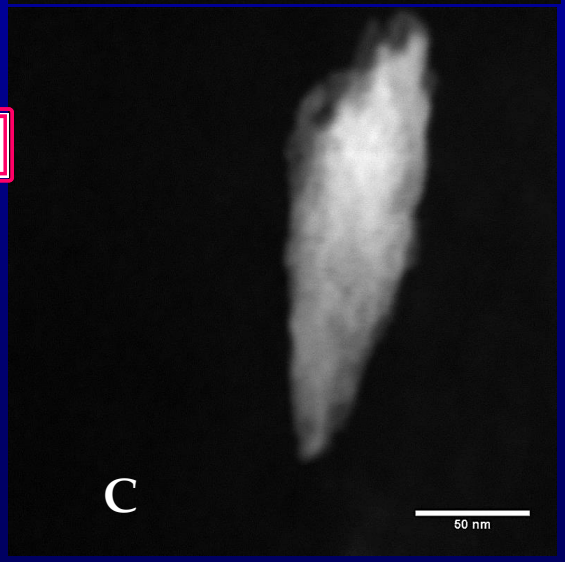

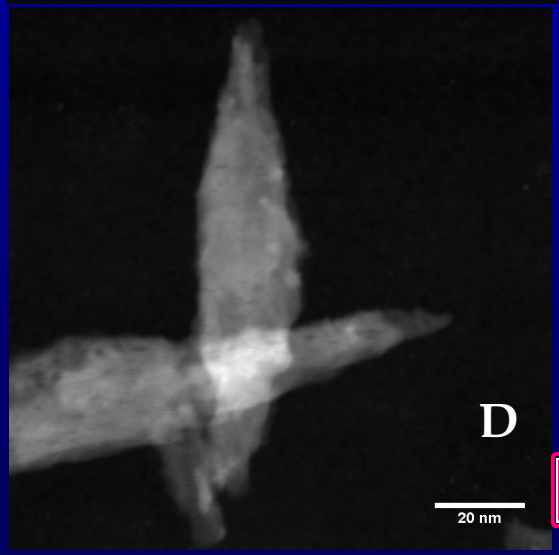

FeHA3

STEM pictures of FEHA (A and B), FeHA2 (C) and FeHA3 (D) at increasing magnification.

FeHA and FEHA2 DC magnetization measurements #1 : Hysteresis loops

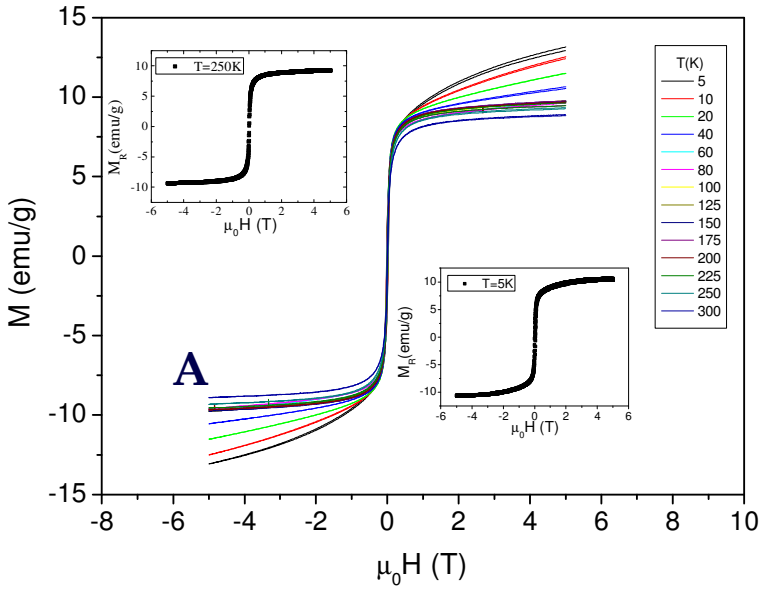

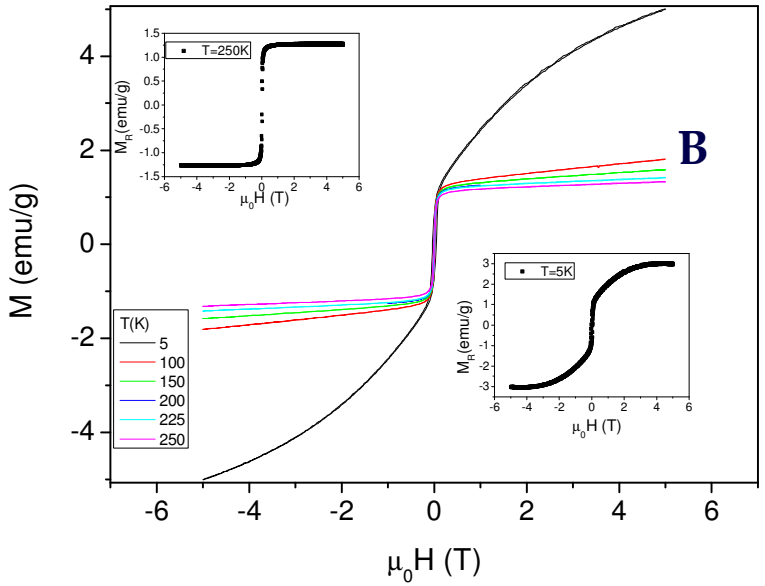

The saturation magnetization values for the magnetically ordered phase were 9.3 and 1.3 emu/g at RT for FeHA (A) and FeHA2 (B), respectively, as well as 10,5 and 2.9 emu/g at 5 K, respectively, obtained by subtracting the linear paramagnetic contribution from the magnetization curves.

Ms of 7–22 emu/g is reported adoptable for bioapplications [JMMM 225, 113-117 (2001), JACS 126, 3392-3393 (2004)]

FeHA DC magnetization measurements

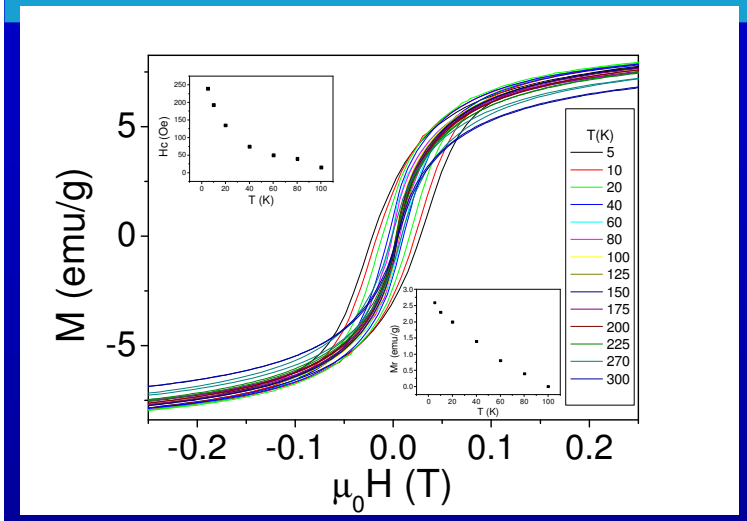

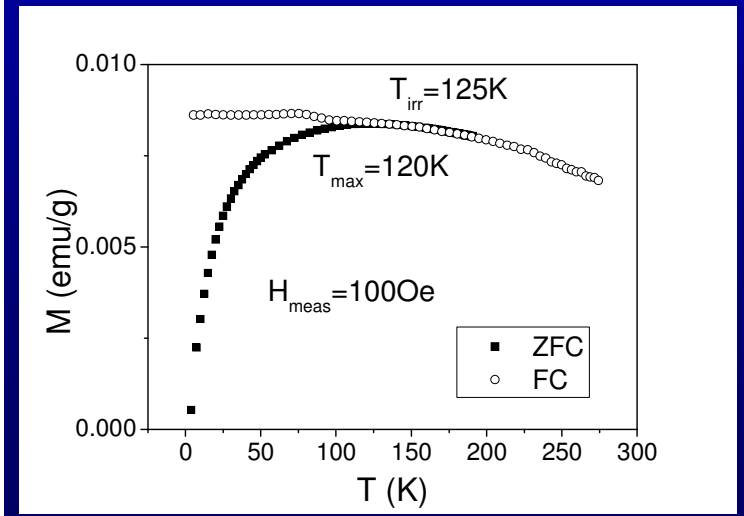

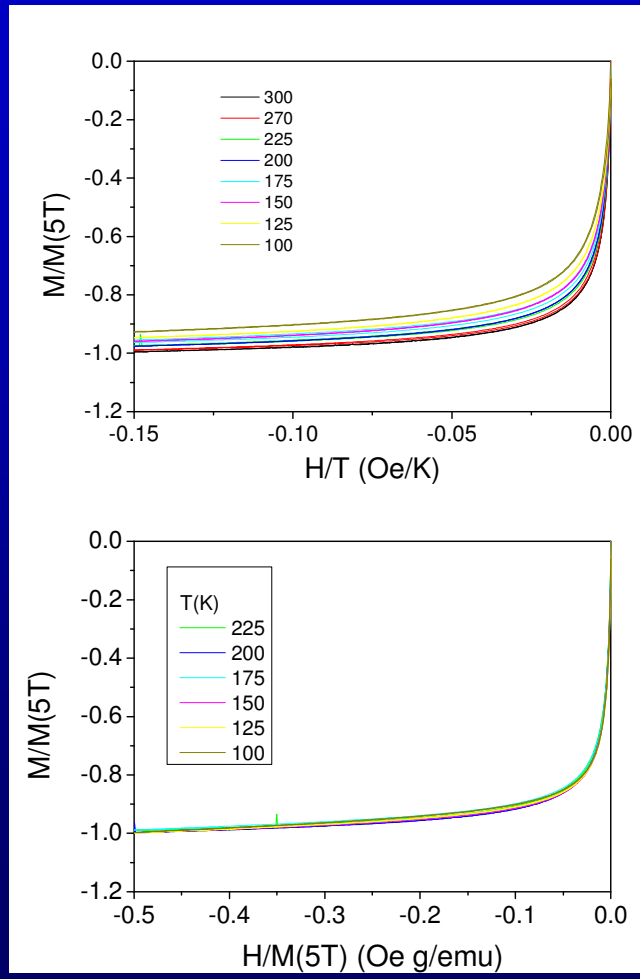

Evidence of nonsuperparamagnetic behavior of the FeHA powder: the standard superparamagnetic scaling law of M/Ms as a function of H/T is not satisfied below 270 K; instead, M/Ms scales as H/Ms (ISP scaling law).

FeHA3 DC magnetization measurements

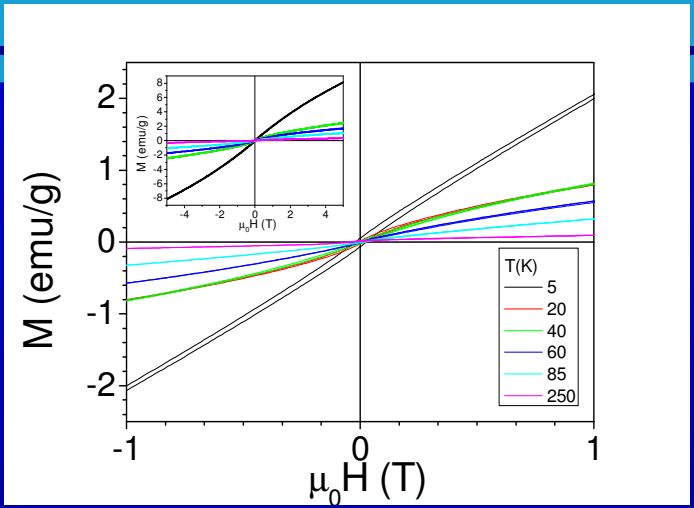

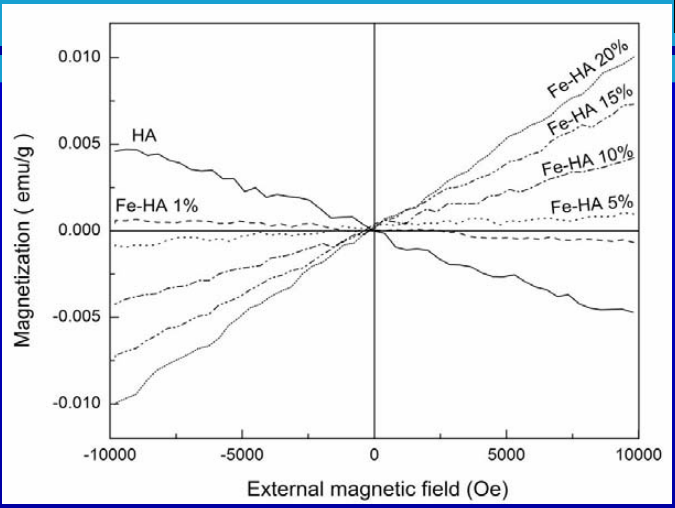

Journal of Physics: Conference Series **187 (2009) 012024, Yan Li, Chai Teck Nam and Chui Ping Ooi**

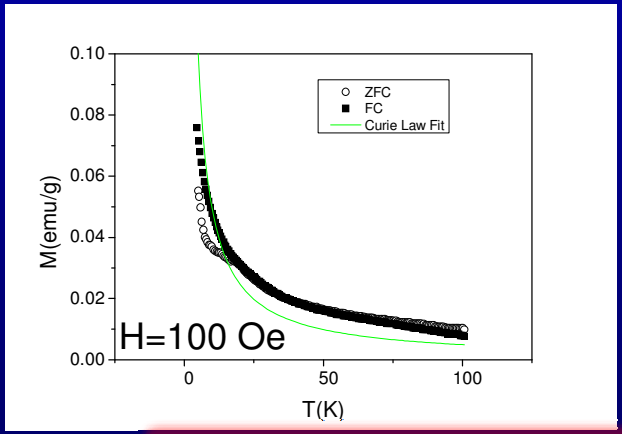

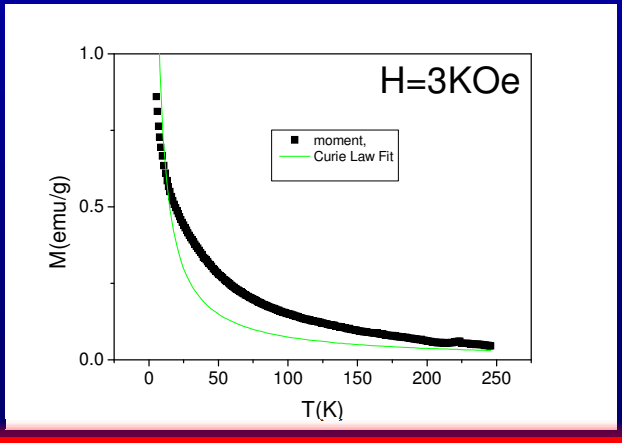

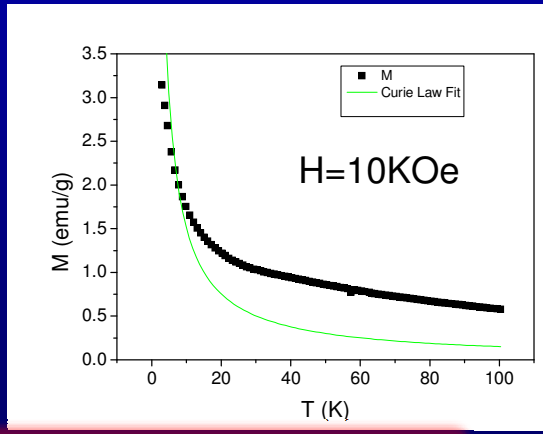

A paramagnetic state exists up to very high fields and over a large temperature range.

An irreversibility between the FC and the ZFC branches of the susceptibility is also observed, in agreement with the hystersis loop.

^{57}Fe MÖSSBAUER SPECTRA on the SAMPLE FeHA At 3K and 292 K

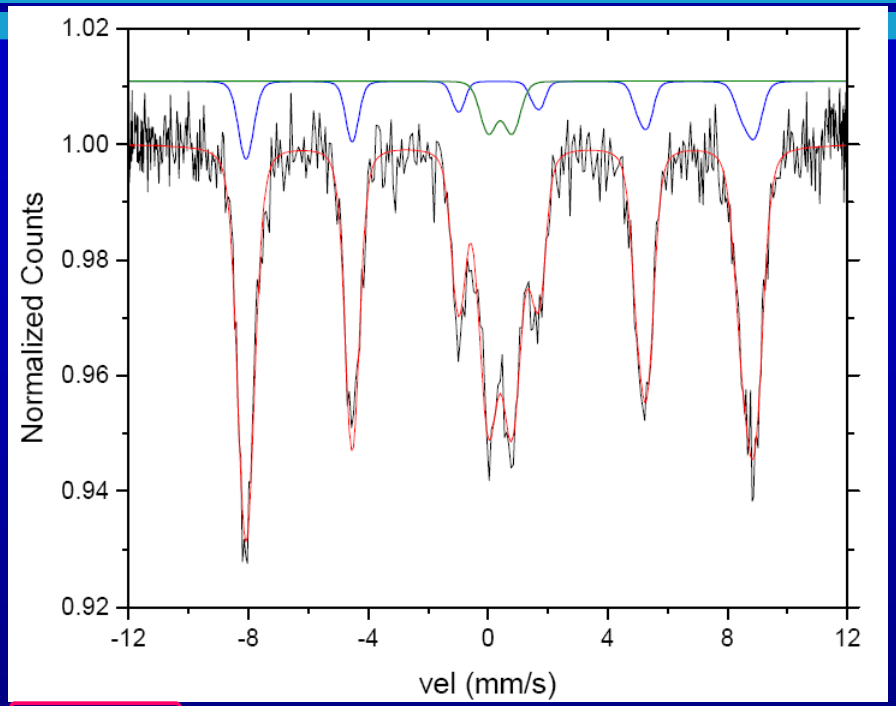

T = 3 K

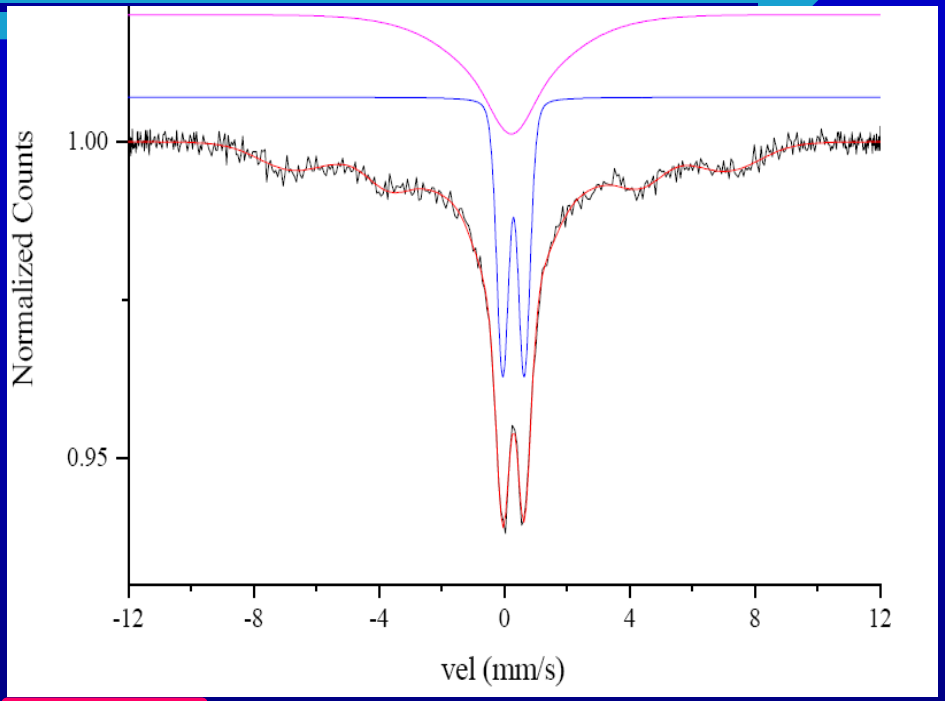

T = 292 K

The Mössbauer spectra at 3K exhibit a) a broad hyperfine spectrum with hyperfine fields of 51.7 and 52.7 T, and b) and a well-defined doublet. Component a) is associated with a magnetically-ordered iron phase that correspond to maghemite. The Mössbauer spectra at room temperatura indicates that the maghemite is poorly-crystallized at room temperature. Component b) is associated with paramagnetic iron. Fits give the relative proportions of these two components: 74% and 26% correspond to component a) and b), respectively.

FeHA MAGNETIC DATA

If we consider that in the sample FeHA the magnetically-ordered iron phase is 74%, we have:

f (wt %)	T (K)	Ms (A m²/Kg)	Ms ^{corr} (A m²/Kg)	Ms ^{corr}/*f* (A m²/Kg)	Ms ^{Fe2O3} (A m²/Kg)
8.82 %	5	10.5	14.2	161	**113**
	250	9.3	12.6	142	**100**

Ms ^{corr} = saturation magnetization corresponding to the magnetically-ordered iron phase equal to 100%.

Magnetic properties of nearly defect-free maghemite nanocrystals

P. Dutta, A. Manivannan, and M. S. Seehra*
Physics Department, West Virginia University, Morgantown, West Virginia 26506-6315, USA

N. Shah and G. P. Huffman
Consortium for Fossil Fuel Science, University of Kentucky, Lexington, Kentucky 40506, USA
(Received 19 April 2004; revised manuscript received 10 August 2004; published 17 November 2004)

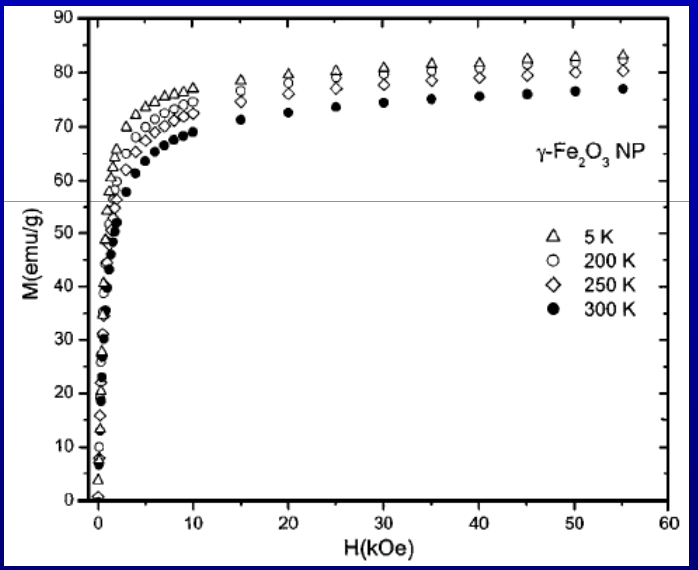

A. Millan et al [JMMM 312, L5-L7 (2007)] showed a variation of saturation magnetization with particle size in maghemite nanoparticles due to the existence of a disordered spin layer at their surfaces, with values in the range 8 - 50 emu/g for nanoparticles sizes in a size range of 3.5-15 nm respectively, although they have shown a high crystalline perfection after annealing.

For the samples FeHA the values of Ms^{Fe2O3} reported in table aren't reasonable values for maghemite.

Biological evaluations

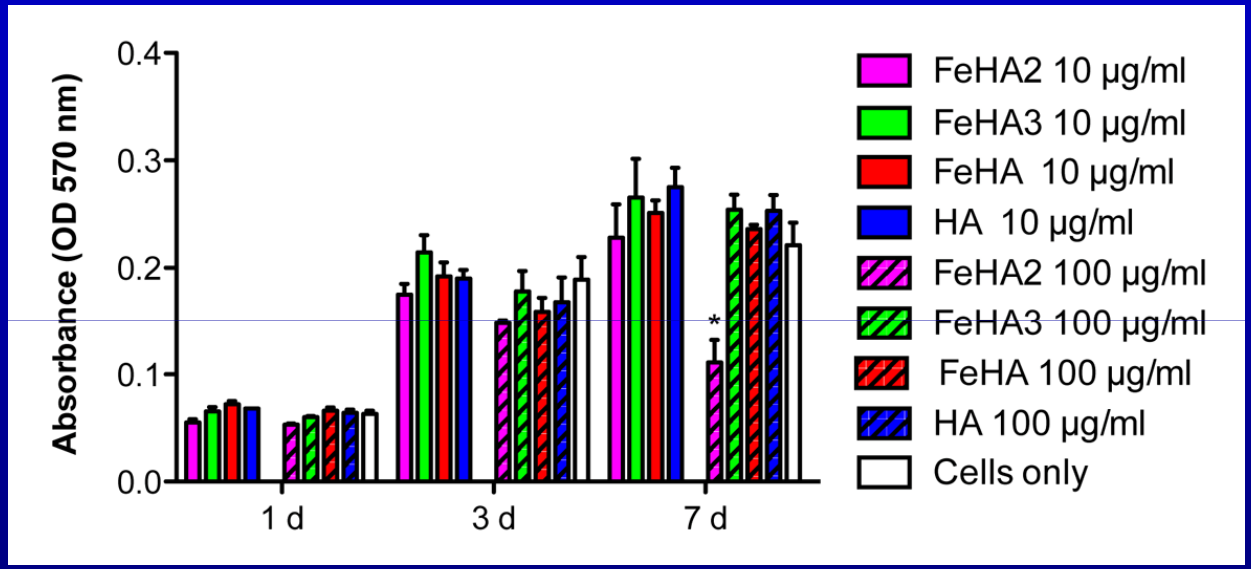

FeHA was found to be fully biocompatible on fibroblast cells, while the administration of FeHA2 produced serious adverse effects on Balb/3T3 cells

CONCLUSIONS

1. We have observed persistent strong paramagnetic behaviour in FEHA3, and a gradual emergence of the interacting superparamagnet regime of a NP system, for T < 270 K in FEHA;

2. In this way it's possible to tune the magnetic properties controlling the oxidation state of iron, through the iron salt used during the wet-chemical synthesis;

3. FeHA was found to be fully biocompatible on fibroblast cells, while the administration of FeHA2 produced serious adverse effects on cells viability;

4. As Ms of 7–22 emu/g is reported adoptable for bioapplications, the level of Ms achieved for FEHA nanoparticles (about 10 emu/g) is deemed sufficient for such applications, exceeding the value for γ-Fe2O3 nanoparticles with the same wt fraction of Fe.

5. The experimental results collectively suggest as regards the FEHA nanoparticles that we have fabricated a magnetic biomaterial, and importantly reducing the amount of iron oxide that would be introduced into the body for biomedical applications but with superior magnetic performance.

Thank you for your attention!

FeHA Monte Carlo model #1

To study the macroscopic behaviour of an assembly of Fe doped hydroxyapatite NPs, with randomly oriented magnetic moments, the particles of the assembly are placed inside a cubic box of edge lengths *Lx*,*Ly*,*Lz*, on the nodes of a simple cubic lattice, with lattice characteristic length α. The box dimensions are *Lx* =*Ly* = *Lz* = 15 measured in units of α.

The whole lattice

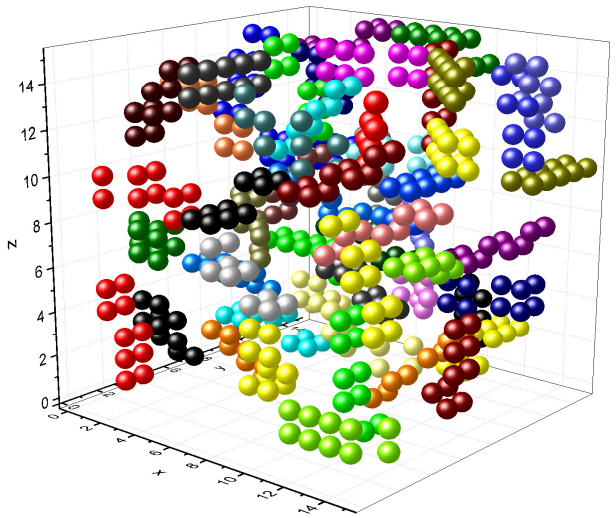

A 3D representation of a sub-cube

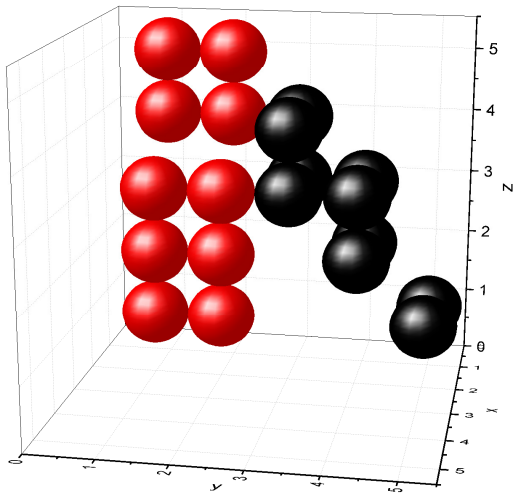

The different colors of the nanoparticles, represent different hydroxyapatite particle. In each smaller box are placed two hydroxyapatite particles with dimensions approximately 5x2x1.

Each hydroxyapatite particle is represented as a randomly oriented array with dimensions 5x2x1 consisted of 10 crystals. Each crystal has spherical shape and diameter *D*. The magnetic crystal are single-domain and represented as three-dimensional classical unit spin vectors. To each crystal an uniaxial easy axis is assigned, randomly distributed in the sample.

FeHA Monte Carlo model #2

The total energy of the system is

$$E = \sum_i E_i$$

where E_i is the energy per particle and is given by the sum of a Zeeman term (due to interaction with an external field), an anisotropy term, and a dipole-dipole interaction (DDI) term:

$$E_i = -\mu_0 m_i H(\vec{s}_i \hat{e}_h) - K_1 V_i (\vec{s}_i \hat{e}_i)^2 - \frac{\mu_0 m_i}{4\pi\alpha^3} \sum_{i>j} m_j \vec{s}_i D_{ij} \vec{s}_j$$

where <i,j> denotes summation over nearest neighbors only, $\hat{e}_h$ and $\hat{e}_i$ are the directions of magnetic field the anisotropy axis of i-th particle. The parameters are the magnetic field H, and the anisotropy constant per unit volume K_1. The thermal energy is denoted $E_T=k_BT$. Finally, $D_{ij,\,ab}$, is the dipolar interaction tensor.

FeHA Monte Carlo model #3

Experiment

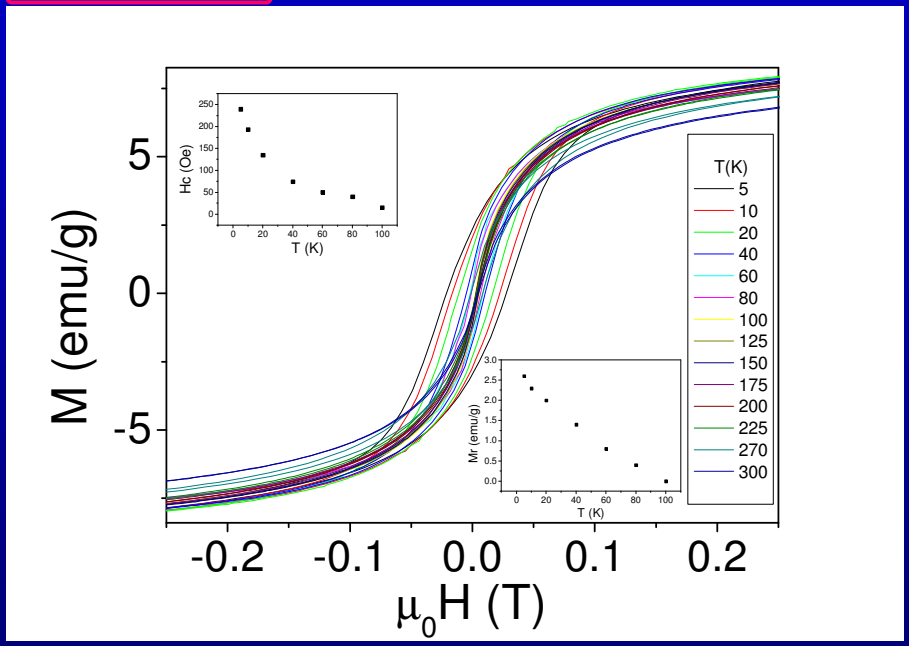

Modeling

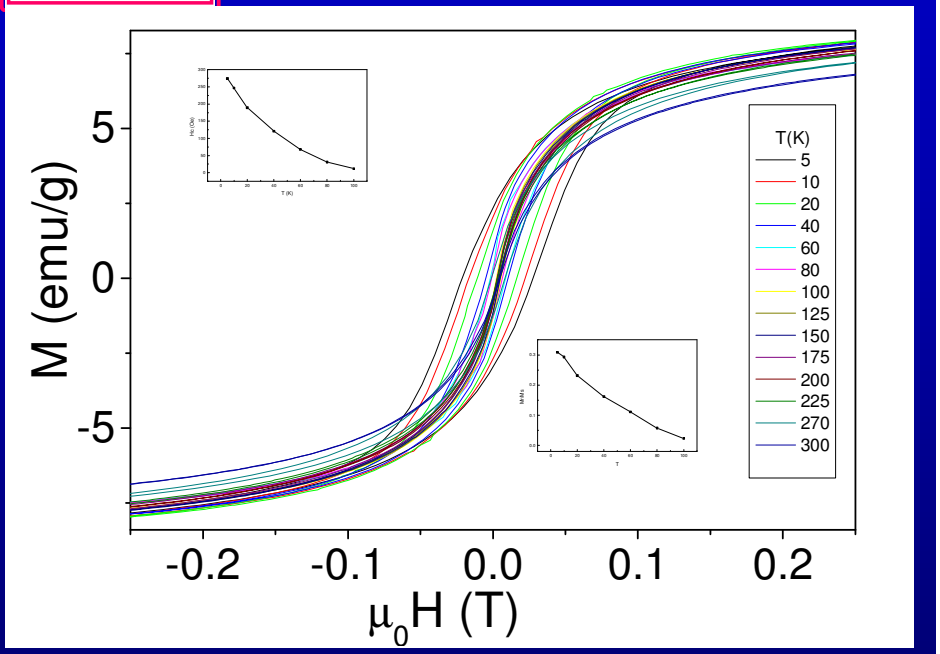

FeHA Monte Carlo model #4

Experiment

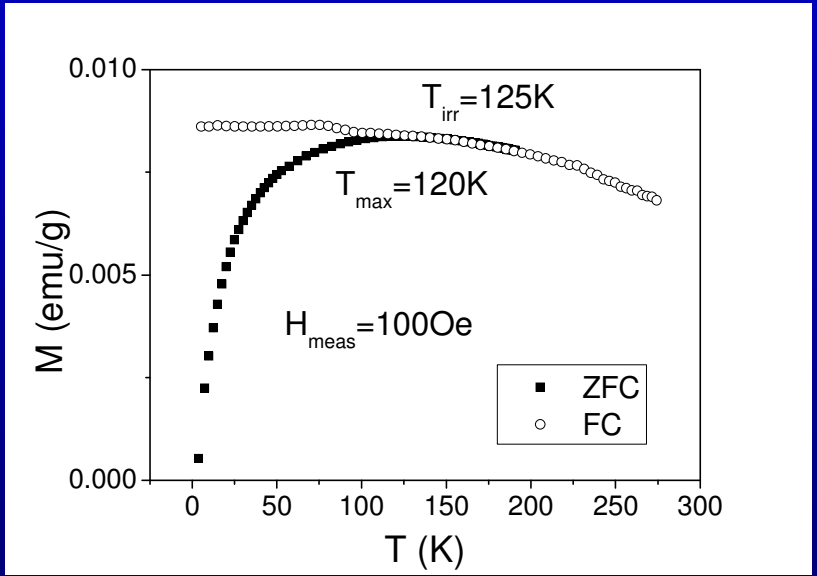

Modeling